The Monomer–Dimer Equilibria of *N*-Hydroxyethylethylenediaminetriacetatovanadium(III) [V(HEDTA)]

Frank J. Kristine and Rex E. Shepherd*

Contribution from the Department of Chemistry, University of Pittsburgh, Pittsburgh, Pennsylvania 15260. *Received March 17, 1977*

Abstract: Electronic spectra and the equilibria for formation of the V(III, III) dimers of $HEDTA^{3-}$ and $EDTA^{4-}$ are reported. The pK_a's and dimerization constants (pK_D, dimerization from two aquo monomers; pK_d, dimerization from two hydroxy monomers) have been determined at $\mu = 0.20$ and 1.00 $NaClO_4$, 25.0 °C, for species at equilibrium with $VL(H_2O)^{1-n}$ (L = $HEDTA^{3-}$, $n = 1$; L = $EDTA^{4-}$, $n = 2$): $pK_a = 6.59 \pm 0.05$; 9.57 ± 0.05, $pK_D = 9.16 \pm 0.02$; 15.99 ± 0.02, $pK_d = -4.01 \pm 0.07$; -3.14 ± 0.07 at $\mu = 1.00$. $[enH_2][(HEDTA)VOV(HEDTA)]\cdot H_2O$ was isolated. The salt exhibits no antiferromagnetic coupling ($S = 2$) in the solid state (Faraday method) or in solution (NMR method) where between pH 3 and 10 the effective moment was 2.75–2.82 μ_B/V(III). Equilibria between the oxo-bridged structure, $LVOVL^{n-}$ (I), a dihydroxy structure $LV(OH)_2VL^{n-}$ (II), and hydroxy-aquo bridged moiety $LV(OH)(OH_2)VL^{(1-n)}$ (VI) are required for the kinetic parameters determined for formation of the V(III, III)(HEDTA) dimer and for its monomerization by a preequilibrium hydrogen ion pathway (type 1). A kinetically indistinguishable hydrogen ion assisted rupture of strained structures of equivalent composition (type 2) is possible. Monomerization of V(III, III) (HEDTA) proceeds at $\mu = 0.20$, 25.0 °C, with $k_1 K_{hyd} = 4.0\ s^{-1}$ and $k_2 K K_{hyd} = 2.51 \times 10^3\ M^{-1}\ s^{-1}$ (type 1) with a preassociation constant for H_3O^+, $K = 7.8\ M^{-1}$. The acid-catalyzed path exhibits activation parameters of $\Delta H^{\ddagger} = 14.5 \pm 0.1$ kcal/mol, $\Delta S^{\ddagger} = -11.3 \pm 3$ eu, $\mu = 0.20$. Formation of the V(III, III)-(HEDTA) dimer occurs with $k_{-1} = 360 \pm 10\ M^{-1}\ s^{-1}$ via hydroxy monomers and $k_{-2} = 428 \pm 30\ M^{-1}\ s^{-1}$ via a hydroxy and an aquo monomer and $25\ M^{-1}\ s^{-1}$ through a separate diaquo path. The kinetics and solution structure of V(III, III) ions are discussed with respect to the $[Fe(HEDTA)]_2O^{2-}$ complex.

A considerable interest exists in inorganic, geochemical, and biochemical disciplines for the μ-oxo-bridged polymeric clusters and hydroxy polymers of tripositive ions. Examples of the simple aquo ion species include the $Al_2(OH)_2^{4+}$, $CrOCr^{4+}$, VOV^{4+}, and $Fe_2(OH)_2^{4+}$ cations. We recently communicated the observation of a V(III) binuclear complex formed either by the inner-sphere electron transfer reaction between $V(HEDTA)^-$ and $VO(HEDTA)^-$ or by a slower association of 2 mol of V(HEDTA) formed by the outer-sphere component of the same cross-reaction.[1,2] The inner-sphere path has allowed detection of a precursor complex of transitory existence having the oxidation state assignment (II, IV). Intramolecular electron transfer within the precursor complex produces a (III, III) dimer, $(HEDTA)VOV(HEDTA)^{2-}$. Analogous Fe(III) binuclear ions of the EDTA family ($EDTA^{4-}$, $HEDTA^{3-}$, $CyDTA^{4-}$) have been characterized by the studies of Walling and Gray,[3] Schugar, Anson, and Gray,[4] and the early explorations of Gustafson and Martell.[5]

The $(HEDTA)FeOFe(HEDTA)^{2-}$ complex is antiferromagnetically coupled with $S = 1$.[3] The formation and dissociation of these binuclear complexes are important as models for inorganic polymerization processes. The association and monomerization steps for the $[Fe(EDTA)]_2O^{4-}$ and $[Fe(HEDTA)]_2O^{2-}$ dimers have been studied by Wilkins and Yellin[6] and by Martell's group.[7] The dominant kinetic pathway for the Fe(III) dimers appears to involve dehydration of an intermediate formed by the combination of aquo and monohydroxy monomer complexes.

No oxo or dihydroxy binuclear complexes of the EDTA family of ligands have been detected for Cr(III) in spite of the well-known tendency of the simple ammine complexes of Co(III) and Cr(III) to form bridged binuclear structures.[11,12] Dihydroxy structures are common for the Co(III) ammines. A binuclear NTA complex $K_2[Co_2(NTA)_2(OH)_2]$ is known and the acid-dependent monomerization has been studied.[39,40]

The Fe(III) EDTA series of complexes were considered as early models for ferritin and as excellent spectral models for hemerythrin.[8] Hemerythrin is a binuclear iron O_2 carrier that uses only protein side-chain residues for binding two Fe(II) centers in close proximity. The biological function of the related hemovanadin is less certain.[9] A complex of the formula $V(C_{16}H_{17}N_3O_{11})(SO_4)_2^{3-}$ can be isolated from cytolysis of vanadocytes. The low molecular weight organic ligand binds four of the coordination sites on the V(III) center.[10] Swinehart et al. have characterized the oxidation state of vanadium found in tunicates from California coastal waters. The oxidation state in the cells of *Ascidia ceratodes* is V(III).[43] Members of the order of Aplousobranchia have predominantly V(IV) in the intact cells.[43] Kustin et al. have found that the cellular blood of *Ascidia nigra* collected in Bermuda waters has vanadium in the III oxidation state.[44] Attempts to isolate the V(III) protein are frequently accompanied with production of EPR-active VO^{2+}. Ehrenberg and Boeri obtained a yellow-brown lysate solution from tunicate cell; the absorbing material is most likely to be a hydrolytic dimer of V(III).[45] Kustin's blood spectrum from *Ascidia* exhibits maxima at about 280 and 335 nm.[44] The spectrum is not similar to that of the known V(III) complexes and it would be useful to have spectra of V(III) complexes in various ligand fields, particularly the N_2O_4 and N_3O_3 donor atom set, for comparison. Swinehart has observed a nonprotein fraction from chromatographed *Ascidia certodes* plasma which reduces V(V) to V(III). Because tunicates must convert vanadates from sea water to its usable V(III) form, the interconversion of various oxidation states of vanadium attached to chelating ligands is of interest. The (III, III) dimer of this report may be generated by a redox path and the vanadium(III) monomers may be obtained by acid-catalyzed cleavage of the dimers. The issue is germane since the cellular organelles which have the highest concentration of V(III) also contain high levels of H_3O^+ (~0.10 M). These findings from the vanadocyte chemistry stimulate an interest in the binding of V(III) to polydentate ligands, particularly those which leave one or two readily exchangeable coordination positions for solvent or other small molecule donors.

The similarities of the Fe(III) and V(III) systems and the novelty that the V(III) dimer may be formed by a redox path has prompted us to characterize the monomeric and dimeric species of the general formulas $VL(H_2O)^{1-n}$, $VL(OH)^{n-}$,

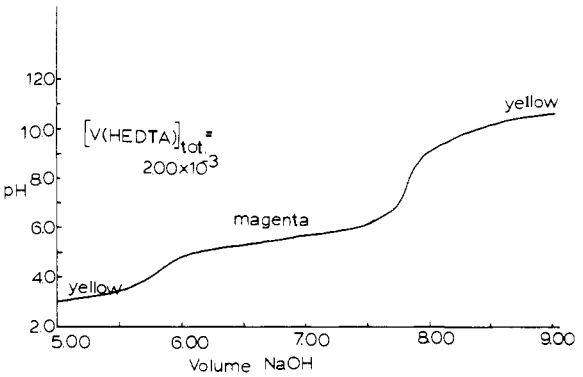

Figure 1. Titration of V(HEDTA)(H_2O) with NaOH, $[V(III)]_{tot} = 2.00 \times 10^{-3}$ M, $\mu = 0.20$, $T = 25.0$ °C, [NaOH] = 0.0486 M.

Table I. Wavelength Maxima and Molar Absorptivity Data for $VL(H_2O)^{1-n}$ and $LVOVL^{2n-}$ Species

L	Species	λ_{max}, nm (ϵ, M^{-1} cm^{-1})[a]		
$HEDTA^{3-}$	Monomer	454 (21.8)	530 (12.6)	
$EDTA^{4-}$	Monomer	454 (27.8)	535 (10.0)	
$DTPA^{5-}$	Monomer	460 (27.4)	533 (17.7)	
$HEDTA^{3-}$	Dimer	469 (28.1)	559 (27.4)	760 (20.3)
$EDTA^{4-}$	Dimer	406 (30.5)	492 (41.1)	708 (16.5)

[a] ϵ/V(III).

$LVOVL^{2n-}$, and $VL(OH)_2^{(n+1)-}$ (L = $EDTA^{4-}$, $n = 2$; L = $HEDTA^{3-}$, $n = 1$). These species have been prepared in solution from VCl_3 as an authentic source of V(III) rather than by the indirect redox route.[1] The hydrogen ion dependencies for dimer association and dissociation are presented in this report. The (III, III) dimer has been isolated as a solid of the formulation $[enH_2][(HEDTA)VOV(HEDTA)]\cdot H_2O$. The solid exhibits no antiferromagnetic coupling as determined by the Faraday method. The Evan's NMR method shows that the dimer is also paramagnetic with $S = 2$ in solution. The magnetic properties of the weakly coupled V(III) centers of the (III, III) dimer are likely to be of theoretical interest.[46a] The low-temperature moments and the structural arrangement of the (III, III) complex will be the subject of a separate report.[46b]

Results

Dimer Equilibria and Spectra. The equilibria shown in eq 1-6 are observed when stoichiometric amounts of VCl_3 and H_3HEDTA or Na_2H_2EDTA are titrated under an inert atmosphere. Similar equilibria occur for the corresponding Fe(III) complexes.[3,5] The oxo-bridged formulation has been selected for the reasons cited in the Discussion section and because of the existence of the analogous $(H_2O)_5VOV(H_2O)_5^{4+}$ ion.

$$V(H_2O)_6^{3+} + L^{(2+n)-} \overset{K_f}{\rightleftharpoons} VL(H_2O)^{1-n} \quad (1)$$

$$VL(H_2O)^{1-n} + H_2O \overset{K_a}{\rightleftharpoons} VL(OH)^{n-} + H_3O^+ \quad (2)$$

$$2VL(H_2O)^{1-n} + 2H_2O \overset{K_D}{\rightleftharpoons} LVOVL^{2n-} + 2H_3O^+ \quad (3)$$

$$2VL(OH)^{n-} \overset{K_d}{\rightleftharpoons} LVOVL^{2n-} + H_2O \quad (4)$$

$$VL(H_2O)^{1-n} + VL(OH)^{n-} \overset{K_dK_a}{\rightleftharpoons} LVOVL^{2n-} + H_3O^+ \quad (5)$$

$$VL(OH)^{n-} + 2H_2O \overset{K_a'}{\rightleftharpoons} VL(OH)_2^{(n+1)-} + H_3O^+ \quad (6)$$

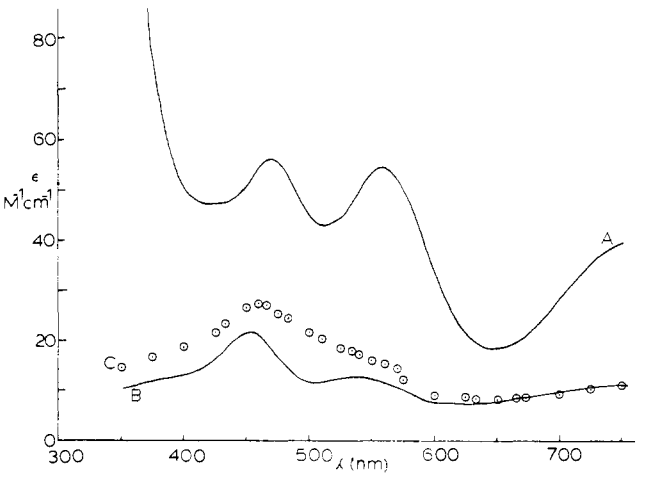

Figure 2. Ultraviolet-visible absorption spectra: (A) $[(HEDTA)V]_2O^{2-}$, pH 5.97; (B) $[(HEDTA)V(H_2O)]$, pH 2.34; (C) $[(DTPA)V]^{2-}$, pH 6.62 ($\mu = 0.11$ $NaClO_4$, $T = 25.0$ °C).

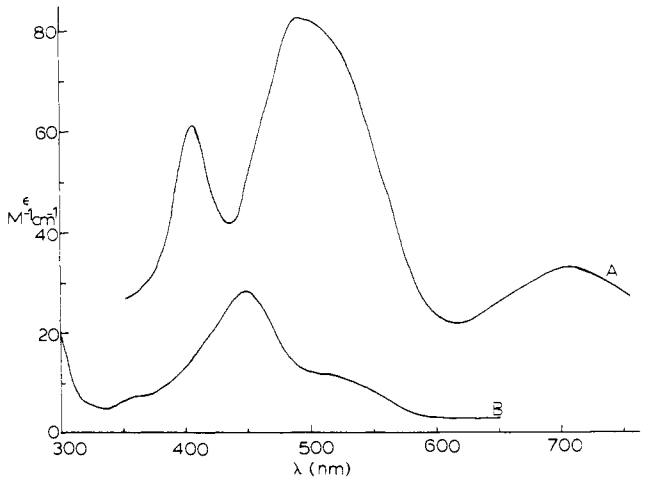

Figure 3. Ultraviolet-visible absorption spectra: (A) $[(EDTA)V]_2O^{4-}$, pH 10.96; (B) $[(EDTA)V(H_2O)^-]$, pH 3.40 ($\mu = 0.10$, $T = 25.0$ °C).

A typical titration curve obtained as described in the Experimental Section is shown in Figure 1. Initially only the dark yellow monomeric complexes, $VL(H_2O)^{1-n}$ and $VL(OH)^{n-}$, species are detected. With increasing pH the magenta $LVOVL^{2n-}$ species is formed. The dimer equilibria shift in favor of $VL(OH)_2^{(n+1)-}$ only at high pH; the solution returns to a yellow brown hue as equilibrium 6 predominates at high pH. The spectra of the monomeric $VL(H_2O)^{1-n}$ and the corresponding $LVOVL^{2n-}$ species (Table I) are shown in Figures 2 and 3 for L = $HEDTA^{3-}$ and L = $EDTA^{4-}$, respectively. Spectra are recorded in the pH domain where either the monomer or dimer is the only species of appreciable concentration in solution. The monomer complexes have very approximate octahedral ligand fields. The 454-nm band of the monomer appears to be split by the lowered symmetry in the $LVOVL^{2n-}$ dimer. The ϵ's per V(III) of the dimer species do not exceed a factor of 2 for those of the monomer species. Transitions in $[V(HEDTA)]_2O^{2-}$ occur shifted by about 65 nm to lower energy from those of the same bands in $[V(EDTA)]_2O^{4-}$. It may be inferred that the higher electrostatic field of $EDTA^{4-}$ relative to $HEDTA^{3-}$ causes a larger ligand field for $EDTA^{4-}$. The Fe(III) dimers have electronic spectra which have been interpreted as two high-spin Fe(III) centers in approximately octahedral coordination.[13]

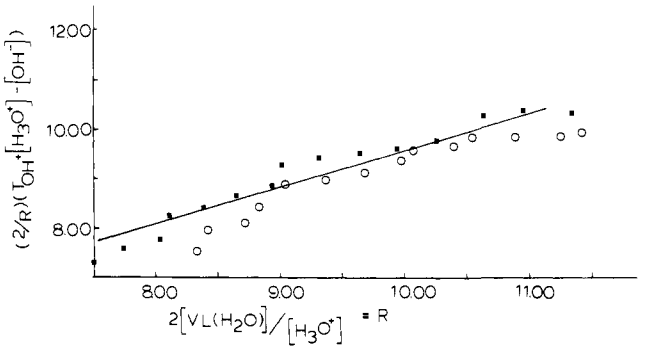

Figure 4. Titration data from V(HEDTA) system: $\mu = 1.00$, $T = 25.0$ °C. ■ and ○ represent separate experiments.

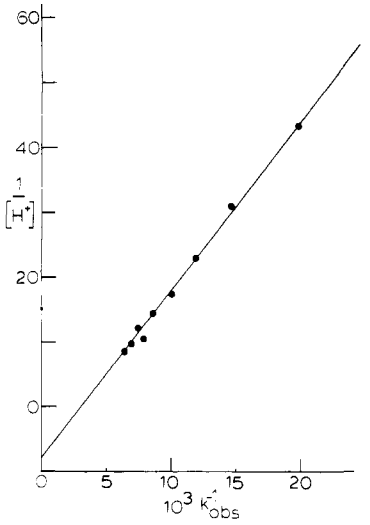

Figure 5. Acid monomerization rate data treated by eq 11.

Combination of the equilibria 1-6 together with mass balance and charge balance expressions provides

$$[VL(H_2O)^{1-n}] = T_M - T_{OH} - [H_3O^+] + [OH^-] \quad (7)$$

$$\frac{[H_3O^+](T_{OH} + [H_3O^+] - [OH^-])}{[VL(H_2O)^{1-n}]} = K_a + \frac{2K_D[VL(H_2O)^{1-n}]}{[H_3O^+]} \quad (8)$$

$$\log K_d = 2pK_a - pK_D \quad (9)$$

where T_M represents the total V(III) concentration in all forms, and T_{OH} is the concentration of NaOH added beyond the formation of the $VL(H_2O)^{1-n}$ monomeric complex.[5] A plot of

$$\frac{[H_3O^+](T_{OH} + [H_3O^+] - [OH^-])}{[VL(H_2O)^{1-n}]} \text{ vs. } \frac{2[VL(H_2O)^{1-n}]}{[H_3O^+]}$$

will yield a straight line of slope K_D and intercept K_a. Potentiometric titration data at 25.0 °C, $\mu = 0.20$ and 1.00, were obtained for $HEDTA^{3-}$ and $EDTA^{4-}$ systems of V(III) under N_2. Representative data for the V(HEDTA) system are shown in Figure 4 at $\mu = 1.00$. The accumulated equilibrium constants that have been determined by this technique are listed in Table II with the existing data for Fe(III) dimers. Values for the pK_a of reaction 2 where the V(III) is replaced by other tripositive cations are given in Table III.

Kinetics of the Monomerization Process. Dissociation of $[V(HEDTA)]_2O^{2-}$ was induced by mixing solutions of the fully formed dimer with solutions of varying hydrogen ion at constant ionic strength ($\mu = 0.20$, $T = 25.0$ °C). The disappearance of the dimer absorbance at 557 nm was monitored in a stopped-flow spectrophotometer. The decrease in absorbance obeys first-order kinetics in $[dimer]_{tot}$ and an apparent saturation effect in $[H_3O^+]$. The data for the monomerization reaction are given in Table IV. These data conform to a $1/[H_3O^+]$ vs. $1/k_{obsd}$ linear dependence as shown in Figure 5. The general mathematical form for k_{obsd} that is implied by this relationship is given by

$$k_{obsd} = \frac{a + b[H_3O^+]}{1 + c[H_3O^+]} \quad (10)$$

The solution structure of the (III, III) dimer is still uncertain as to whether the V(III) centers are joined by an oxo ligand or by dihydroxy bridging ligands (see the Discussion section). Since (III, III) is produced by the intramolecular electron transfer bleaching of (II, IV), the oxo structure must exist at least as a kinetic transient. The reverse reaction of (III, III) monomerization exhibits a rate term dependent on two molecules of the hydroxy monomer and it is certain that the dihy-

Table II.[a] Hydrolytic Equilibrium Constants for V(III) and Fe(III) Complexes of $HEDTA^{3-}$ and $EDTA^{4-}$

	V(HEDTA)	V(EDTA)$^-$	Fe(HEDTA)	Fe(EDTA)$^-$
pK_a	6.59 ± 0.05	9.57 ± 0.05	4.11 ± 0.07[c]	7.58[d]
	6.39 ± 0.10[b]	10.16 ± 0.01[b]		
pK_D	9.16 ± 0.02	15.99 ± 0.02	5.84 ± 0.01	12.21
	9.05 ± 0.02[b]	16.71 ± 0.01[b]		
pK_d	−4.01 ± 0.07	−3.14 ± 0.07	−2.38 ± 0.08	−2.53
	−3.74 ± 0.10[b]	−3.62 ± 0.02[b]		

[a] $\mu = 1.00$, $T = 25.0$ °C. [b] $\mu = 0.20$, $T = 25.0$ °C. [c] References 3, 5. [d] Reference 4.

Table III. Acid Dissociation Constants for Monomeric Complexes of $M(III)L(H_2O)^{1-n}$

	Ionic radii		pK_a		
M(III)	Pauling	Shannon-Prewitt	HEDTA	EDTA	Ref
Ru		0.70		7.63	42
V	0.74	0.64	6.59 ± 0.10	10.2	This work
Rh	0.68	0.67		9.2	14
Cr	0.63	0.62	6.13 ± 0.10	7.39 ± 0.03	15
Mn	0.66	0.65	3.7[a]	5.5[a]	16
Fe	0.64	0.65	4.11 ± 0.07	7.58	4,5
Co	0.63	0.53		~8	17
Al	0.51	0.53		5.92	18

[a] May be coordination number 7.

Table IV. Data from the Hydrogen Ion Induced Monomerization of $(HEDTA)VOV(HEDTA)^{2-}$[a]

$[H_3O^+]$	k_{obsd}	$1/k_{obsd} \times 10^3$	$1/[H_3O^+]$	$k_{obsd}(1 + K_2[H_3O^+])$
0.115	158	6.33	8.70	300.
0.102	144	6.94	9.80	259.
0.0951	126	7.94	10.5	219.
0.0820	135	7.41	12.2	221.
0.0690	121	8.26	14.5	186.
0.0620	107	7.94	16.1	159.
0.0520	98.8	10.0	19.2	139.
0.0436	84.7	11.8	22.9	114.
0.0321	69.0	14.5	31.1	86.3
0.0229	50.8	19.7	43.7	59.8

[a] $\mu = 0.20$ $NaClO_4$, $T = 25.0$ °C; average of three or more runs, $K_2 = 7.79$ M^{-1}.

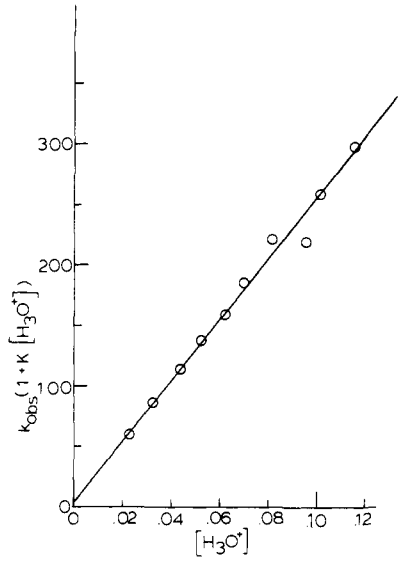

Figure 6. Acid monomerization rate data treated by eq 12.

droxy structure also exists at least as a kinetic transient. The two species differ only by the components of a solvent molecule and the hydration equilibrium 11 accounts for the intercon-

$$\underset{\text{I}}{\text{LMOML}^{2-}} + \text{H}_2\text{O} \overset{K_{hyd}}{\rightleftharpoons} \underset{\text{II}}{\text{LM}(\text{OH})_2\text{ML}^{2-}} \qquad (11)$$

version. Two kinetic pathways are compatible with the general law of eq 10. These include the following: (1) preequilibrium protonation catalysis (eq 12-14) and (2) proton-assisted rupture of a strained system (eq 15-17).[47] In these general schemes D represents the (III, III) either as structure I or II and D* represents a strained bond structure of the (III, III) dimer. Structures III, IV, and V readily come to mind as

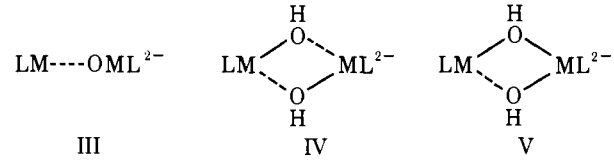

III IV V

strained structures which would be susceptible to proton-assisted rupture.

Type 1

$$\text{D} + \text{H}_3\text{O}^+ \overset{K_{12}}{\rightleftharpoons} \text{DH}^+ + \text{H}_2\text{O} \qquad (12)$$

$$\text{D} \xrightarrow{k_{13}} \text{monomers} \qquad (13)$$

$$\text{DH}^+ \xrightarrow{k_{14}} \text{monomers} \qquad (14)$$

Type 2

$$\text{D} \underset{k_{-15}}{\overset{k_{15}}{\rightleftharpoons}} \text{D}^* \qquad (15)$$

$$\text{D}^* \xrightarrow{k_{16}} \text{monomers} \qquad (16)$$

$$\text{H}_3\text{O}^+ + \text{D}^* \xrightarrow{k_{17}} \text{monomers} \qquad (17)$$

The protonation preequilibrium path is shown in Scheme I for the dihydroxy structure (II); for an oxo bridged species

Scheme I

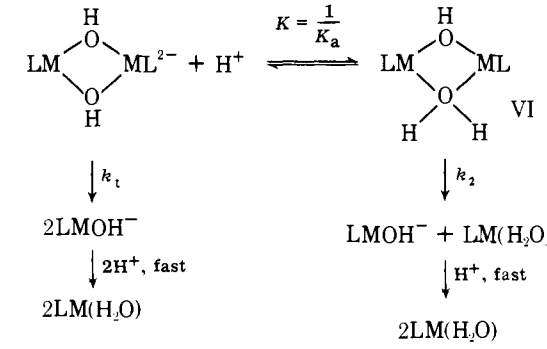

Scheme II

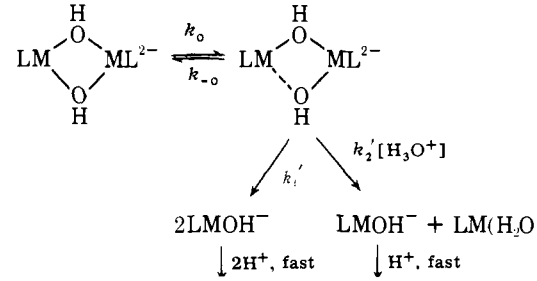

(I) addition of H_2O may occur concerted with k_1 or k_2 steps which break the dimer structure. Similarly, the proton-assisted rupture of a strained system is shown in Scheme II with structure V with the potentially concerted hydration of III as an equivalent path.

Application of the usual mass balance and equilibrium equations to Scheme I (type 1) yields expression 18. Application of mass balance equations, the steady-state approximation on the concentration of D*, and the assumption that the pseudoequilibrium constant (k_0/k_{-0}) favors structure D yields eq 19 for Scheme II (type 2). The steady-state and $(k_0/k_{-0}) \ll 1$ is essential to provide a first-power dependence in $[H_3O^+]$ in the denominator of eq 19 with $K' = k_0/(k_{-0} + k_1')$.

$$\frac{1}{[\text{LMOML}]_{tot}} \frac{d[\text{LMOML}]}{dt} = \frac{k_1 + k_2 K[H_3O^+]}{1 + K[H_3O^+]} \qquad (18)$$

$$\frac{1}{[\text{LMOML}]_{tot}} \frac{d[\text{LMOML}]}{dt} = \frac{K'(k_1' + k_2'[H_3O^+])}{1 + K'\left(\frac{k_2'}{k_0}\right)[H_3O^+]} \qquad (19)$$

The implication of coefficients a, b, and c from eq 10 is easily seen by inspection of eq 18 and 19 for the respective general mechanisms of type 1 and type 2. The linear fit of the data in Figure 5 implies that $a/[H_3O^+] < b$ in eq 20 for $[H_3O^+] > 0.02$ M.

$$\frac{1}{[H_3O^+]} = \frac{1}{k_{obsd}}\left(\frac{a}{[H_3O^+]} + b\right) - c \qquad (20)$$

The intercept, c, is determined as 7.8 M^{-1} from Figure 5. The slope, 2.64×10^3 M^{-1} s^{-1}, serves as an initial estimate of b although a refinement is obtained from eq 21 with c taken to be 7.8 M^{-1}.

$$k_{obsd}(1 + c[H_3O^+]) = a + b[H_3O^+] \qquad (21)$$

The monomerization data in the form of eq 21 are shown in Figure 6. The values of a and b are established as 4.0 s^{-1} and 2.51×10^3 M^{-1} s^{-1}, respectively. The validity of the statement $a/[H_3O^+] \ll b$ for $[H_3O^+] > 0.02$ M is established; $a/[H_3O^+]_{max} < 200$ M^{-1} s^{-1} or <8% of b. The relative efficiencies of the acid-catalyzed path to the uncatalyzed dissociation are given by $(b/a) = 628$ for the type 2 systems and $(b/Ka) = 81$ for type 1 systems.

Table V. Dimer Formation in the Presence of Buffers at $\mu = 0.20$, $T = 25.0$ °C

k_{obsd}	pH	Buffer system	$10^{11}k_{obsd}(K_a^2 + 2K_a(H_3O^+) + (H_3O^+)^2)$
78.8	5.35	*a*	172.7
194	6.53	*a*	5.92
199	6.84	*b*	3.21
277	7.21	*c*	2.81
271	7.23	*c*	2.70
310	7.49	*b*	2.60
339	7.77	*b*	2.54
315	7.80	*c*	2.42
347	7.96	*c*	2.49
373	8.28	*c*	2.57
384	8.31	*c*	2.54
311	8.78	*c*	2.08
345	8.80	*c*	2.31
348	8.90	*c*	2.32
366	9.01	*c*	2.44
393	9.03	*c*	2.62

[a] $HPO_4^{2-}/H_2PO_4^-$ buffer. [b] 2,6-Lutidine/2,6-lutidinium ion buffer. [c] Tris(hydroxymethyl)aminomethane buffer.

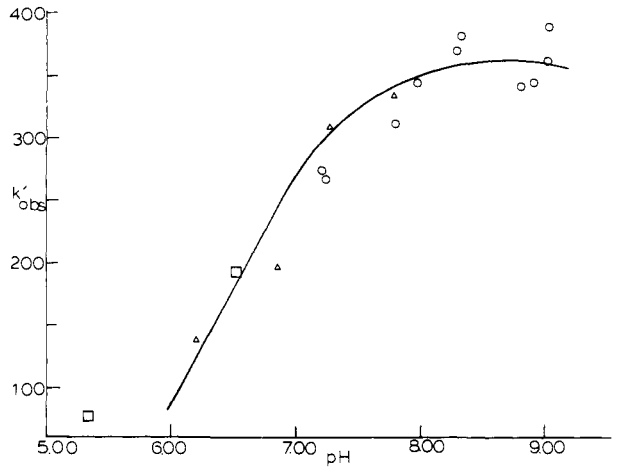

Figure 7. pH profile of V(HEDTA) dimer formation: □, phosphate buffer; Δ, 2,6-lutidine buffer; ○, Tris buffer ($\mu = 0.20$, $T = 25.0$ °C).

Kinetics of Dimer Formation. Formation of the dimer from V(HEDTA)(H_2O) monomer solutions was monitored in the stopped-flow device by means of the pH-jump method at 557 nm. V(HEDTA)(H_2O) was rapidly mixed with appropriate buffers at $\mu = 0.20$, $T = 25.0$ °C. The pH domain of 5.35–9.03 was covered with phosphate, 2,6-lutidine, and tris(hydroxymethyl)aminomethane buffers. The data obtained under various conditions are given in Table V and a pH profile of k_{obsd} from the second-order reaction in $[V(III)monomer]_{tot}$ appears in Figure 7.

Overlapping buffer regions were used to show that no specific buffer effects were noticed in the value of k_{obsd} for 2,6-lutidine, phosphate, or Tris buffers. The lutidine buffer runs were affected in the initial part of the reaction by the heat of dilution of the buffer. A specific buffer effect in the pH range of 8–9 was observed for borate or mannitol-borate buffers. The rates were very slow in the presence of the borate systems. The value of k_{obsd} remained nearly constant at 23 ± 1 M^{-1} s^{-1} from pH 8.3 to 8.9. Comparison to the Tris buffer data reveals a larger rate suppression in mannitol-borate buffer. It seems likely that borate ion complexes with V(HEDTA) and that removal of $B(OH)_4^-$ or a carboxylate chelate ring opening becomes rate determining. The rate constant for dimer formation in the presence of the other buffer systems reaches a limiting value under hydrogen ion conditions which exceed by more than 2 pK units the pK_a of V(HEDTA)(H_2O) (see Figure 7 and Table II). The law of microscopic reversibility would require the reverse reaction of Schemes I or II for reformation of the dimer complex to proceed via the dihydroxy bridged intermediate (II) and the hydroxy-aquo intermediate (VI) or through distorted structures III, IV, or V. Assuming that the formation of intermediates by either scheme are rate limiting from two hydroxy monomers or an aquo and a hydroxy monomer, respectively, the sequence for dimer formation given by eq 22 and 23 is most likely.

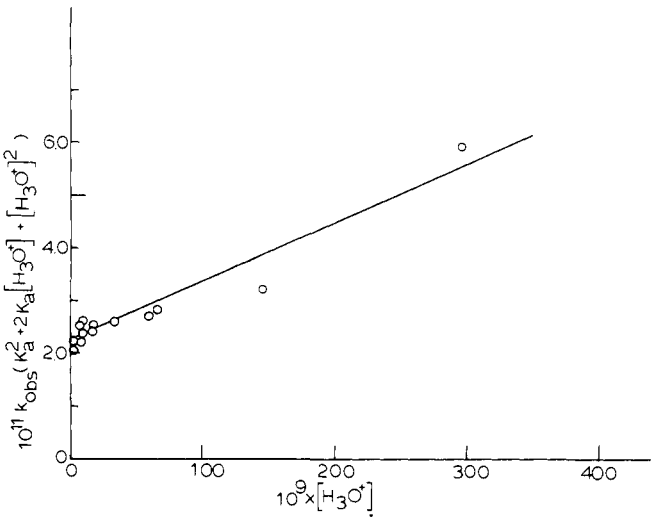

Figure 8. V(HEDTA) dimer formation data treated by eq 16.

$$VL(OH)^- + VL(OH)^- \xrightarrow{k_{-1}} LVOVL^{2-} + H_2O \quad (22)$$

$$VL(OH)^- + VL(H_2O) \xrightarrow{k_{-2}} LVOVL^{2-} + H_3O^+ \quad (23)$$

Equation 24 may be derived from the mass balance expression, K_a, and Scheme II.

$$\frac{d[LVOVL^{2-}]}{dt} = \frac{k_{-2}K_a[H_3O^+] + k_{-1}K_a^2}{(K_a^2 + 2K_a[H_3O^+] + [H_3O^+]^2)} \times (VL(H_2O))^{tot}_{monomer})^2 \quad (24)$$

$$k_{obsd}' = \frac{k_{-2}K_a[H_3O^+] + k_{-1}K_a^2}{(K_a^2 + 2K_a[H_3O^+] + [H_3O^+]^2)} \quad (25)$$

Equation 25 may be rearranged in a linear form having a slope of $k_{-2}K_a$ and intercept $k_{-1}K_a^2$ illustrated by Figure 8. The values obtained by this method are $k_{-2} = 428$ M^{-1} s^{-1} and $k_{-1} = 345$ M^{-1} s^{-1}. The solid line shown in the pH profile of Figure 7 is obtained by using p$K_a = 6.59$, $k_{-1} = 360 \pm 10$ M^{-1} s^{-1}, and $k_{-2} = 428 \pm 30$ M^{-1} s^{-1}. These values provide the best agreement for eq 25 in the pH range above 6.0. Only the data point at pH 5.35 is substantially deviant from the theoretical curve (solid line). This is anticipated because the hydroxy monomer is only 0.05% of the total monomer concentration. The mechanism shifts to the association of two aquo monomers. This path is represented by eq 26 with $k_{-3} \simeq 25$ M^{-1} s^{-1}.

$$VL(H_2O) + VL(H_2O) \xrightarrow{k_{-3}} LVOVL^{2-} + 2H_3O^+ \quad (26)$$

Monomerization Activation Parameters. The temperature dependence was studied at 0.0436 M in H_3O^+ from 11.0 to 29.8 °C ($\mu = 0.20$). The data are presented in Table VI. The fit of the data to the Eyring rate expression is shown in Figure 9. Under these conditions the acid-independent path (a) contributes only 4% of the observed rate. The activation parameters are found to be $\Delta H^{\ddagger} = 14.5 \pm 0.1$ kcal/mol and $\Delta S^{\ddagger} = -11.3 \pm 3$ cal/mol K and these are taken to be the activation parameters of the acid-catalyzed path (b).

Table VI. Temperature Dependence of Acid-Catalyzed Monomerization[a]

Temp, °C	k_{obsd}, s^{-1}	$1/T \times 10^3$	$-\ln(k_c/T)$
284.2	30.3	3.519	2.289
286.6	34.7	3.489	2.111
288.2	38.5	3.470	2.013
291.5	50.7	3.431	1.749
296.6	76.2	3.372	1.359
298.4	84.7	3.351	1.260
301.6	97.0	3.316	1.134
302.8	113.	3.303	0.986
303.0	110.	3.300	1.013

[a] $\mu = 0.20$ $NaClO_4$.

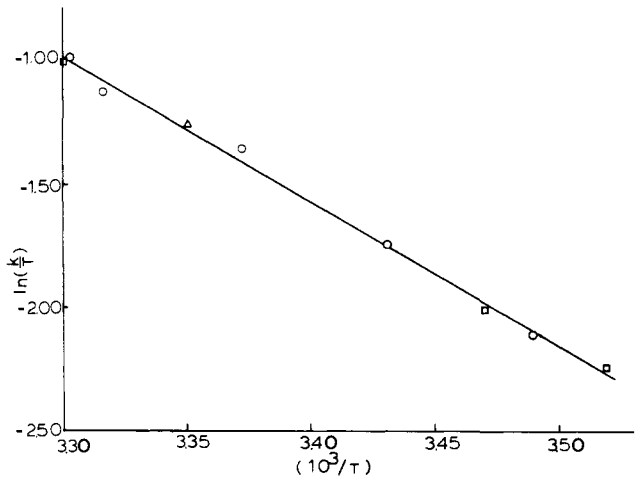

Figure 9. Temperature dependence of acid-catalyzed monomerization.

Magnetic Studies of (HEDTA)VOV(HEDTA)$^{2-}$. The solution magnetic moment was determined by dissolving $[enH_2][(HEDTA)VOV(HEDTA)]\cdot H_2O$ in 2% *tert*-butyl alcohol-H_2O solution. The pH was 6.5 in the domain where the dimer is fully formed (see Figure 1). The solution gram susceptibility was determined vs. an internal capillary butanol reference at 313 K by the Evans' NMR method.[19] Diamagnetic corrections were calculated using Pascal's constants.[20] The corrected molar magnetic susceptibility, χ_M^{corr}, was found to be 3.03×10^{-3} cgs units per V(III). The effective magnetic moment was calculated from the Curie law (eq 27) to be 2.75 μ_B/V(III). Similar experiments from pH 3 to 10 gave values in the range of 2.75–2.82 μ_B. The spin-only value for a d^2 V(III) center is 2.83. The monomeric V(HEDTA)(H_2O) complex gave a value of 2.82 μ_B for μ_{eff} at 296 K by the same procedures.

$$\mu_{eff} = 2.828\sqrt{\chi_{corr}T} \qquad (27)$$

The solid $[enH_2][(HEDTA)VOV(HEDTA)]\cdot H_2O$ was examined by the Faraday method with $Hg[Co(SCN)_4]$ as the reference compound. A corrected molar magnetic susceptibility χ_m^{corr} of 3.18×10^{-3} cgs units/V(III) was found at 297 K. The Curie law evaluates μ_{eff} as 2.75 μ_B/V(III) for the dimer in the solid state. These studies indicate that $S = 2$ for the (III, III) dimer both in solution and the solid state.

Infrared Vibrational Spectra. Nujol mull spectra were obtained for $[enH_2][(HEDTA)VOV(HEDTA)]\cdot H_2O$ and $Na[V(EDTA)(H_2O)]$. The vibration at about 850 cm^{-1} usually attributed to the M-O-M stretching frequency is virtually absent.

Hendrickson reports the absence of any strong band in the 800–900 cm^{-1} region for an Fe(III)-Fe(IV) oxo-bridged porphyrin[48b] and Gray has reported the absence of this band in a Mn-O-Mn porphyrin of Mn(III).[48a] Meyer et al. could find no IR-active bands in this region for $Cl(bipy)_2RuORu(bipy)_2Cl^{n+}$ complexes.[48c] Other IR-active bands for the vanadium complexes are shown in Figure 10.

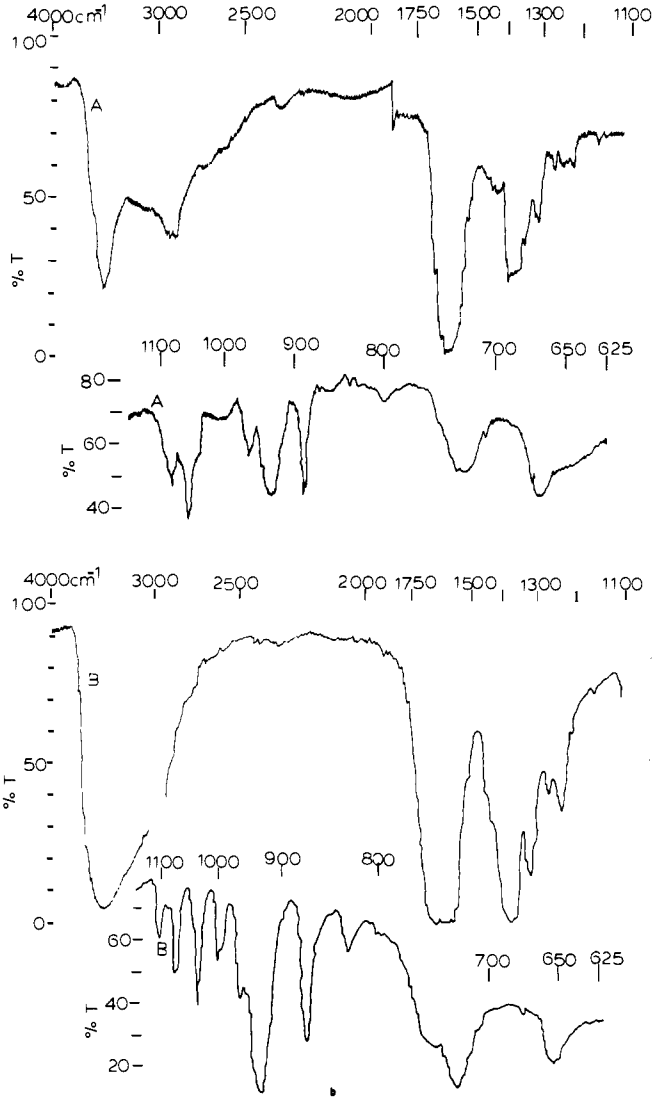

Figure 10. Infrared spectra in KBr pellets: (A) $[enH_2][(HEDTA)VOV(HEDTA)]\cdot H_2O$, (B) $Na[V(EDTA)(H_2O)]$.

Conclusions

Nature of the Dimer Species. The existence of monomer-dimer equilibria for V(III)(HEDTA) and V(III)(EDTA)$^-$ is confirmed by the titration data, electronic spectra, and isolation of the dimer as $[enH_2][(HEDTA)VOV(HEDTA)]\cdot H_2O$. Magnetic studies on the dimer in solution and in the solid state show the dimer to have four unpaired electrons ($S = 2$). The V(III) dimer does not show antiferromagnetic coupling as is present in the Fe(III) dimer. There is no strong IR band near 850 cm^{-1} which is usually assigned to the M-O-M stretching frequency. However, this frequency can no longer be accepted as proof of the absence of this structure.[48] The medium band at 880 ± 10 cm^{-1} is also detected for the $Na[V(EDTA)(H_2O)]$ monomer salt. The absence of any free carboxylate functionalities with a different vibration from those of coordinated groups supports structure I. The aquo V(III) dimer has been attributed to be the dihydroxy bridged structure[21] although the cation is generally considered to be the oxo-bridged VOV^{4+} ion.[22] Dimeric complexes of V(III) in solution for the *o*-phenanthroline[23] and terpyridine[24] have been postulated as $(phen)_2V(OH)_2V(phen)_2^{4+}$ and $(trpy)V(OH)_2V(trpy)^{4+}$. The magnetic moment data for $(HEDTA)VOV(HEDTA)^{2-}$ are consistent with either

structure I or II. A molecular orbital description similar to ones already attributed[3,25] to $Cl_5RuORuCl_5^{4-}$, $(NH_3)_5CrOCr(NH_3)_5^{4+}$, and (HEDTA)FeOFe(HEDTA)$^{2-}$ would assign four electrons from the oxo bridge and four electrons from the two V(III) centers to populate two bonding and three effectively degenerate nonbonding orbitals: $(E_u{}^b)^4[E_g{}^2B_{2g}{}^1B_{2u}{}^1]E_u{}^*$. The dihydroxy structure is also consistent with the absence of superexchange which would lower the effective moment below 2.8 μ_B/V(III).

A species of at least transitory existence having a composition with the oxo-bridged structure I may be inferred from the formulation of the highly absorbing V(II, IV) dimer.[2] If structure II is the dominant solution form of the (III, III) dimer, then hydration must be rapid relative to intramolecular electron transfer. From the collected data it would appear that only a x-ray diffraction study can answer whether structure I or II is the dominant species in the solid state.

The value found for c (7.8 M^{-1}) is in reasonable agreement for a preequilibrium protonation of the dihydroxy structure II based on the value of 42.8 ± 2.7 M^{-1} reported by Meloon and Harris[40] for the (NTA)$Co(OH)_2Co$(NTA)$^{2-}$ complex. In Scheme I the constant c equals the protonation constant, K. For Scheme II the constant, c, equals $K'(k_2'/k_0) = (k_2'/k_{-0} + k_1')$. The ratio $(k_2'/k_1') = 628$; if competition occurs for the strained intermediate D* for conversion to monomers and reversion to the D structure, k_{-0} must be competitive with $k_2'[H_3O^+]$ within a factor of 10-100. Under this assumption $(k_{-0} + k_1') \simeq k_{-0}$. Therefore $c \simeq (k_2'/k_{-0})$. If type 2 mechanisms are involved and an estimate of k_2' is taken as the diffusion limited rate of $\sim 10^{11}$ M^{-1} s^{-1} for proton scavenging of D*, the value of c = 7.8 M^{-1} would require k_{-0} to be $\sim 8 \times 10^{11}$ s^{-1}. It follows that $k_0 < 10^{10}$ s^{-1} from the approximation $(k_0/k_{-0}) \ll 1$. Any lower value of k_2' will produce the same relative decrease in k_0. This calculated value of k_0 is much less than a vibrational frequency which suggests that partial bond rupture is present in D* as shown by structures III-V. The values obtained with c = 7.8 M^{-1} are within the realm of possibility. Therefore type 2 behavior cannot be ruled out in preference to type 1 on this basis.

The electrostatically similar V(HEDTA)(H_2O) and Co(NTA)$(H_2O)_2$ species have pK_as of 5.56 and 6.71,[40] respectively. Therefore, V(III) is about 12-fold more acidic than Co(III). An estimate of K of 3.6 M^{-1} is obtained from correcting Harris's equilibrium constant by a factor of 12 for Scheme I. The estimated value is within a factor of 2 of the kinetically determined value of 7.8 M^{-1}.

The protonation effect does not seem to be explained by protonation of a pendant carboxylate group (eq 28). Cr(EDTA)$(H_2O)^-$ has a pK_a for the pendant carboxylate arm of 1.8 ± 0.2.[15] The HEDTA complexes of M(III) species should be more acidic owing to a lower net electrostatic charge. The aquo ligand in M(III)HEDTA complexes is more acidic by 2-4 pK units than in M(III)EDTA(H_2O). A pendant arm should reduce the electrostatic difference. The observed value for pK of 0.8 seems too high for a pendant carboxylate protonation equilibrium involving V(HEDTA)(H_2O) or the (III, III) dimer.[41]

$$LMOML^{2-} + H_3O^+ \overset{k_{28}}{\rightleftharpoons} HO \sim\sim LMOML^- \quad (28)$$

The pK_as for $V(H_2O)_6{}^{3+}$ and $Fe(H_2O)_6{}^{3+}$ are 2.92 and 2.19, respectively.[26] It is anticipated that Fe(III) complexes are more acidic than their V(III) analogues. This fact is illustrated by the data in Table II. The pK_as of V(HEDTA)(H_2O) and V(EDTA)$(H_2O)^-$ are nearly a constant of 2.5 log units higher than the Fe(III) complexes of the same ligands. The equilibrium of the dimer complex with the aquo monomers (eq 3) is less favorable by nearly 3.5 log units for the V(III) system relative to Fe(III); however, the equilibrium involving hydroxy monomers (eq 4) is more favorable for the V(III) system. In each case the dimer formation is more favorable for the HEDTA^{3-} system relative to EDTA^{4-}. This is reasonable because charge repulsions for the monomer fragments within the dimer will be larger in the (EDTA)MOM(EDTA)$^{4-}$ species than in the (HEDTA)MOM(HEDTA)$^{2-}$ complex. Charge repulsions dominate acidities of the monomeric M(HEDTA)(H_2O) and M(EDTA)$(H_2O)^-$ complexes. The pK_as for all of the complexes listed in Table III follow the effective ionic radii assigned to the ion with the exception of Mn(III). Mn(III) may be seven coordinate in its EDTA family complexes[16] which would account for its anomaly in this series. The presence of Al(III) in the proper order and magnitude of its pK_a for the Al(EDTA)$^-$ system shows that the hydrolysis of the transition metal monomers is dominated by the electrostatic component; the pK_a of the EDTA complexes obey a reasonably linear dependence on $1/r$ using the Pauling ionic radii.

Table VII. Kinetic Data for V(III) and Fe(III) Formation and Monomerization

	k_{-1}, M^{-1} s^{-1}	k_{-2}, M^{-1} s^{-1}	k_1K_{hyd}, s^{-1}	$k_2K_{hyd}K$, s^{-1}
V(HEDTA)	3.60×10^2	4.3×10^2	4.0	2.51×10^3
Fe(HEDTA)	9.0×10^2	6.0×10^4	4.0	3.0×10^6
Fe(EDTA)	6.0×10^2	2.0×10^4	1.2	5.0×10^8

Mechanism of Dimer Formation and Dissociation. A comparison of equivalent kinetic pathways for dimer association and dissociation is given in Table VII for V(III) and Fe(III) complexes assuming the mechanism in Scheme I and the prehydration equilibrium of eq 11. The Fe(III) rate constants are those of Wilkins and Yellin determined in 1.0 M $NaNO_3$ medium by the temperature-jump method. Forward and reverse rates for the V(III) system were carried out at μ = 0.20, T = 25.0 °C. The buffer media and acid media for the pH jump procedure are not equivalent and the ratio of the rate constants differs by 90-fold from the static method for the equilibrium constant given in Table III. For the uncatalyzed pathways for both the V(III) and Fe(III) complexes the rate constants are remarkably similar. However, the acid-catalyzed paths (k_{-2} and k_2KK_{hyd}) are slower by about 10^2 for the V(III) system relative to Fe(III) which is approximated by the ratio of the water exchange rates of V(III) and Fe(III) aquo complexes.[27]

Newton and Baker report $\Delta H^{\ddagger}$ = 9.4 kcal/mol and $\Delta S^{\ddagger}$ = −26.1 eu for the VOV^{4+} acid-catalyzed monomerization.[28] The values found for the (HEDTA)VOV(HEDTA)$^{2-}$ monomerization ($\Delta H^{\ddagger}$ = 14.5 kcal/mol, $\Delta S^{\ddagger}$ = −11.3 eu) show that the more negatively charged environment for either the oxo or dihydroxy portion of the HEDTA dimer costs less in entropy terms for protonation than for the VOV^{4+} cation. The activation enthalpies differ by 5 kcal/mol for protonation. Both values are in the range of $\Delta H^{\ddagger}$ of the acid-promoted path for the monomerization of $Fe_2(OH)_2{}^{4+}$ where reported values of 10.5 ± 0.5,[29a] 11.2 ± 0.1,[29b] and 6 ± 2 kcal/mol[29c] at 25 °C, μ = 3.0 $NaClO_4$, are found. That the activation entropy is negative is supportive of structure I as the true solution species. The $\Delta S^{\ddagger}$ values for disruption of $Fe_2(OH)_2{}^{4+}$ and $(Cr(o\text{-phen})_2(OH)]_2{}^{4+}$ are +3[29c] and +0.5 eu,[30] respectively. The negative activation entropies for VOV^{4+} and (HEDTA)VOV(HEDTA)$^{2-}$ support a greater degree of ordering for the activated complex. This would suggest that the (III, III) dimer of V(HEDTA) is likely to be oxo bridged in solution similar to its aquo ion analogue.

The value of 14.5 kcal/mol and the rate constant at 25 °C associated with rupture of structure VI is also close to the rate 1.14×10^2 M^{-1} s^{-1} and $\Delta H^{\ddagger}$ for solvent exchange (13.5 ± 0.8) as deduced by substitution of NCS^- on $V(H_2O)_6{}^{3+}$ [30] The

values shown by k_2KK_{hyd} (3.51×10^3 M^{-1} s^{-1}) are modestly larger, consistent with the labelization of coordinated water by ligands such as $HEDTA^{3-}$. The relative assistance of the H^+-promoted path to the unassisted path for monomerization—628 for V(III) and 7.5×10^5 for Fe(III)—reveals that the V(III) system is less sensitive to H^+ catalysis by 1000-fold. This result is consistent with greater charge repulsion for the protons of coordinated H_2O molecules in the Fe(III) complex which is also displayed by the greater acidity of the monomeric Fe(III) complexes (Table III).

Medium effects obscure the exact relative magnitude of the differences for the V(III) vs. Fe(III) complexes. However, the formation rate constants also follow the trends shown by the monomerization paths. The formation of structure III from two hydroxy monomers is nearly the same for V(III) and Fe(III) (k_{-1} path). The "acid-assisted" formation pathway via intermediate IV is more efficient for the Fe(III) complex by about 100-fold.

The study of the V(III) and Fe(III) dimers with $HEDTA^{3-}$ raises the question as to why the $Cr(HEDTA)(OH)^-$ complex fails to form a similar dimer.[31] Charge factors would seem to be favorable. The monomeric Cr(III) complex is known to be anomalously labile for Cr(III) complexes[15,31] and the reactivity has been attributed to the transitory expansion of the coordination number of Cr(III) to 7 by attack of the pendant hydroxyethyl or acetato arms of $HEDTA^{3-}$ and $EDTA^{4-}$, respectively.[15] It seems likely that the lability of the $Cr(HEDTA)(H_2O)$ complex contributes to the instability of the dimer complex of Cr(III). The slow substitution rate for the Co(III) complex and the preference for ring closure to form the sexidentate monomer complex[17] would seem to be the origin of the lack of the dimeric species for Co(III)(HEDTA). Work is in progress on the Mn(III)HEDTA complex to examine the effect of 7 coordination on potential dimer equilibria for the Mn(III) system.[32]

The spectra obtained for the monomer and dimer complexes of $EDTA^{4-}$ and $HEDTA^{3-}$ for V(III) show little similarity to the plasma spectrum of the tunicates as found by Kustin. The $DTPA^{5-}$ complex shows only slight differences from the $HEDTA^{3-}$ spectrum. Its coordination for the 1:1 V(III):$DTPA^{5-}$ would appear to involve only the terminal and middle N donors with their respective acetato groups as ligands for V(III). The iminodiacetate fragment would appear to remain uncoordinated; a similar result is observed for the 1:1 spectrum of $VO(DTPA)^{3-}$ which is essentially unchanged from that of $VO(HEDTA)^-$. The N_2O_4 and N_3O_3 donor series appear to be unrelated to the tunicate spectrum. It is possible that the small extinction coefficients of V(III) octahedral complexes could be masked by other components in the *Ascidia* blood. Given the opportunity, V(III) would seem to prefer N_2O_4 rather than N_3O_3 based on the $DTPA^{5-}$ monomer complex spectrum. It is quite possible that the V(III) complex in tunicate cells is bound in a site with fewer than six ligand donors; a series of five coordinate complexes with N_2O_3 and N_3O_2 environments is under study in our laboratory as potential binding analogues of the *Ascidia* V(III) complex.

Experimental Section

The stopped-flow experiments were conducted on a Durrum D-110 spectrophotometer. V(III) solutions were manipulated under N_2 which was purified through Cr(II) bubblers and supplied to glass vessels via an all-glass manifold. Solutions were manipulated by syringe techniques using gas-tight syringes. Titration data were obtained in an N_2 purged cell with a thermostated jacket at 25.0 °C. Potentiometric data were monitored on an Orion 601 digital pH meter standardized with appropriate buffers. N_2-purged NaOH was added with a Gilmont microburet. All spectra were recorded on a Varian-Cary 118C spectrophotometer. IR data were recorded in KBr or Nujol mulls with a Beckman IR8 or Beckman IR Acculab 4 instrument.

VCl_3. VCl_3 was prepared by reduction of V_2O_5 with S_2Cl_2.[34] Workup procedures were carried out in anhydrous conditions within glove bags. Purity of samples was checked for V(IV) by means of the presence or absence of the EPR eight-line VO^{2+} spectrum on a Varian E-4 EPR at room temperature.

$[enH_2][(HEDTA)VOV(HEDTA)]\cdot H_2O$. Equal molar amounts (0.02 mol) of VCl_3 and $H_3(HEDTA)$ were placed in a three-necked flask and purged with N_2. O_2-free solvent water was added with magnetic stirring to dissolve the VCl_3. Ethylenediamine was added until the pH probe in one of the necks indicated pH neutrality. The solution was combined by dropwise addition of dimethylformamide until the solution appeared cloudy. The preparation was flushed with N_2 and stored in a refrigerator overnight. The crystalline powder which was obtained was filtered and washed with dimethylformamide and ether before drying in a vacuum desiccator with pumping. The formulation $[enH_2][(HEDTA)VOV(HEDTA)]\cdot H_2O$ is implied. Anal. Calcd: C, 33.90; H, 5.57; N, 11.07. Found: C, 33.66; H, 5.97; N, 11.84.[33] The solution spectrum was identical with that of the species formed by the titration experiments in situ with NaOH.

$Na[V(EDTA)(H_2O)]$. VCl_3 and Na_2H_2EDTA (0.02 mol each) were combined under N_2 with H_2O. NaOH pellets were added to raise the pH to 6.0. Light brown crystals formed upon cooling in ice. The solid was filtered, washed with cold methanol and cold ether, and dried in a desiccator.[34] Analysis of a weighed sample by means of its electronic spectrum and the known solution ϵ's indicated the formula weight corresponding to only one coordinated H_2O molecule. The sodium salt of $VO(EDTA)^{2-}$ was also isolated from the mother liquor after air oxidation.

Magnetic Data. The Evan s NMR method was used to obtain solution magnetic moment data in H_2O.[35] The probe temperature of the Varian EM360 device was measured by the separation of the CH_3 and OH resonances of methanol.[36] $(CH_3)_3COH$ was used as the reference resonance; it was present in both the (III, III) dimer solution and in an internal capillary. The solid state magnetic data were obtained on a Faraday balance apparatus,[36] using standard techniques.

Reagents. Commercial buffers and ligands were used as supplied. $NaClO_4$ was prepared as a stock solution from a salt recrystallized three times and analyzed by the tetraphenylarsonium perchlorate gravimetric method.[37]

Acknowledgment. We gratefully acknowledge the assistance of the Research Corporation for funds that enabled us to purchase the stopped-flow spectrophotometer and to support these studies.

References and Notes

(1) F. J. Kristine, D. Gard, and R. E. Shepherd, *J. Chem. Soc., Chem. Commun.*, 994 (1976).
(2) Abbreviations: $EDTA^{4-}$ = ethylenediamine *N,N,N',N'*-tetraacetate, $HEDTA^{3-}$ = *N*-hydroxyethylethylenediamine *N,N',N'*-triacetate, $CyDTA^{4-}$ = 1,2-diaminocyclohexane *N,N,N',N'*-tetraacetate.
(3) H. Schugar, C. Walling, R. B. Jones, and H. B. Gray, *J. Am. Chem. Soc.*, **89**, 3712 (1967).
(4) H. J. Schugar, A. T. Hubbard, F. C. Anson, and H. B. Gray, *J. Am. Chem. Soc.*, **91**, 71 (1969).
(5) R. L. Gustafson and A. E. Martell, *J. Phys. Chem.*, **67**, 576 (1963).
(6) R. G. Wilkins and R. E. Yellin, *Inorg. Chem.*, **8**, 1470 (1969).
(7) G. McLendon, R. J. Motekaitis, and A. E. Martell, *Inorg. Chem.*, **15**, 2306 (1976).
(8) I. M. Klotz, G. L. Klippenstein, and W. A. Hendrickson, *Science*, **192**, 335 (1976).
(9) N. M. Senozan, *J. Chem. Educ.*, **51**, 503 (1974).
(10) H. J. Bielig, H. D. Dell, H. Mollinger, and W. Rudiger, *Justus Liebigs Ann. Chem.*, **662**, 206 (1963); H. Mollinger, Ph.D. Thesis, University of Frieburg, Germany, 1960.
(11) (a) F. A. Cotton and G. Wilkinson, "Advanced Inorganic Chemistry", Interscience, New York, N.Y., 1972; (b) C. J. Ballhausen, "Ligand Field Theory", McGraw-Hill, New York, N.Y., 1962.
(12) C. L. Rollinson and D. Nicholls in "Comprehensive Inorganic Chemistry", Pergamon Press, Elmsford, N.Y., 1973.
(13) H. J. Schugar, G. R. Rossman, C. G. Barraclough, and H. B. Gray, *J. Am. Chem. Soc.*, **94**, 2683 (1972).
(14) F. P. Dwyer and F. L. Garvan, *J. Chem. Soc. A*, 4823 (1966).
(15) H. Ogino, T. Watanbe, and N. Tanaka, *Inorg. Chem.*, **14**, 2093 (1975).
(16) Y. Yoschino, A. Ouchi, Y. Tsundo, and M. Kojima, *Can. J. Chem.*, **40**, 775 (1962); R. E. Hamm and M. A. Suwyn, *Inorg. Chem.*, **6**, 139 (1967).
(17) J. A. W. Shimi and W. C. E. Higginson, *J. Chem. Soc.*, 260 (1958).
(18) G. Schwartzenbach, R. Gut, and G. Anderegg, *Helv. Chim. Acta*, **37**, 937 (1954).
(19) D. F. Evans, *J. Chem. Soc.*, 2003 (1959); D. Ostfeld and I. J. Cohen, *J. Chem. Educ.*, **49**, 829 (1972).
(20) A. Earnshaw, "Introduction to Magneto-chemistry", Academic Press, New

York, N.Y., 1968.
(21) L. Pajdowski and B. Jezowska-Trzebiatowska, *J. Inorg. Nucl. Chem.*, **28**, 443 (1966).
(22) T. W. Newton and F. B. Baker, *Inorg. Chem.*, **3**, 569 (1964); ref 11a, 12.
(23) W. W. Brandt, F. P. Dwyer, and E. C. Gynarfas, *Chem. Rev.*, **54**, 959 (1954).
(24) L. E. Bennett and H. Taube, *Inorg. Chem.*, **7**, 254 (1968).
(25) (a) S. J. Lippard, H. Schugar, and C. Walling, *Inorg. Chem.*, **6**, 1825 (1967); (b) J. D. Dunitz and L. E. Orgel, *J. Chem. Soc.*, 2594 (1953).
(26) L. G. Sillen and A. E. Martell, "Stability Constants", Publication No. 17, The Chemical Society, London, 1964.
(27) H_2O exchange on V(III) occurs at about 10^3 s^{-1}: private communication for $V(H_2O)_6^{3+}$ exchange from L. Donham and H. Taube. The uncertainty caused by the medium effects on the measured rates precludes a more rigorous comparison.
(28) Reference 22.
(29) (a) B. Lutz and H. Wendt, *Ber. Bunsenges. Phys. Chem.*, **74**, 372 (1970); (b) H. N. Po and N. Sutin, *Inorg. Chem.*, **10**, 428 (1971); (c) B. A. Sommer and D. W. Margerum, *Ibid.*, **9**, 2517 (1970).
(30) D. Wolcott and J. B. Hunt, *Inorg. Chem.*, **7**, 755 (1968).
(31) N. Keder, J. Harner, and R. E. Shepherd, in progress; also ref 15.
(32) J. Nelson and R. E. Shepherd, work in progress.
(33) Analysis by Galbraith Laboratories, Inc.
(34) We thank J. Harner for the isolation of the $Na[V(EDTA)(H_2O)]$ salt.
(35) Presence of 2-methylpyrazine in a similar sample also exhibited dipolar paramagnetic shifts without any apparent competition for the oxo or dihydroxo ligands of the (III, III) dimer.
(36) A. J. Gordon and R. A. Ford "The Chemist's Companion", Wiley, New York, N.Y., 1972.
(37) E. S. Gould and H. Taube, *J. Am. Chem. Soc.*, **86**, 1318 (1964).
(38) M. Mori, M. Shibata, E. Kyuno, and Y. Okubo, *Bull. Chem. Soc. Jpn.*, **31**, 940 (1958).
(39) M. A. Thacker and W. C. E. Higginson, *J. Chem. Soc., Dalton Trans.*, 704 (1975).
(40) D. R. Meloon and G. M. Harris, *Inorg. Chem.*, **16**, 434 (1977).
(41) If K_{28} represents a second solution unreactive form of (III, III), the denominator term becomes $(1 + K[H_3O^+])(1 + K_{28}[H_3O^+])$. Since no marked second-order dependence in $1/[H_3O^+]^2$ is observed one or the other of the product terms is nearly 1.0. Microscopic reversibility would suggest that protonation occurs at a bridging ligand site and similar reactivities are reported for the Fe(III) system without utilizing chelate ring opening as a limiting step. This would imply that constant $c = K$ for Scheme I and that $K \gg K_{28}$.
(42) K. Shimizu, T. Matsubara, and G. Sato, *Bull. Chem. Soc. Jpn.*, **47**, 1641 (1974).
(43) J. H. Swinehart, W. R. Biggs, D. J. Halko, and N. C. Schroeder, *Biol. Bull.*, **146**, 302 (1974).
(44) K. Kustin, D. S. Levine, G. C. McLeod, and W. A. Curby, *Biol. Bull.*, **150**, 426 (1976).
(45) E. Boeri and A. Ehrenberg, *Arch. Biochem. Biophys.*, **50**, 404 (1954).
(46) (a) W. E. Hatfield, private communication. (b) Work in progress: R. E. Shepherd, F. Kristine and W. E. Hatfield at University of North Carolina, Chapel Hill.
(47) We wish to acknowledge a referee who has pointed out that the type 2 mechanism is equally supportable by the data.
(48) (a) R. F. Ziolo, R. H. Stanford, G. R. Rossman, and H. B. Gray, *J. Am. Chem. Soc.*, **96**, 7190 (1974); (b) R. G. Wollmann and D. N. Hendrickson, *Inorg. Chem.*, **16**, 723 (1977); (c) T. R. Weaver, T. J. Meyer, S. A. Adeyemi, G. M. Brown, R. P. Eckberg, W. E. Hatfield, E. C. Johnson, R. W. Murray, and D. Untereker, *J. Am. Chem. Soc.*, **97**, 3039 (1975).

Synthesis and Characterization of Species Containing Three Metal Atoms

Russell S. Drago* and Joel H. Elias

Contribution from the School of Chemical Sciences, University of Illinois, Urbana, Illinois 61801. *Received December 16, 1976*

Abstract: The synthesis of a series of complexes of the general formula $CapCo(dmg)_3Cap^{n+}$, where dmg is dimethylglyoximato and Cap is diethylenetriaminechromium(III); diethylenetriaminecobalt(III); 1,1′,1″-tris(aminomethyl)ethanecobalt(III); triaquonickel(II), diethylenetriaminenickel(II); triaquozinc(II) and diethylenetriaminezinc(II). The proposed structures are supported by elemental analyses, NMR, and conductivity experiments. Magnetic susceptibility studies to 4.2 K indicate little interaction between the unpaired electrons of the paramagnetic capping groups. Electrochemical studies indicate that in contrast to stabilization of the II oxidation state by the BF cap of the clathrochelate $FB[Co(dmg)_3]BF$ the metal caps stabilize the III oxidation state. The cobalt center of the metal capped complexes are even more difficult to reduce than the cobalt in $K_3Co(CN)_6$. ^{59}Co NMR spectra are reported and discussed.

Current interest in heterogeneous and biological catalytic systems which involve the action of more than one metal center has stimulated the synthesis and study of materials containing more than one metal in the ion or molecule. For ease of discussion, such molecules or ions will be referred to as metallomers and the standard prefixes (di-, tri-, etc.) used to indicate the number of metal ions in the species. Before any generalizations can be established regarding the influences that one metal center in a molecule can have on the chemistry at another metal center, a wide variety of soluble materials will have to be prepared in which the factors influencing metal-metal synergism can be varied in a systematic way. This is a report of the synthesis and characterization of a series of complexes that contain three metal ions in the same molecule. The materials are novel in that soluble species can be synthesized in which two of the metals are different from the third.

The trimetallomers in this system are derived from the salt $K_3Co(dmg)_3$ (where dmg represents the dimethylglyoximato anion). The synthesis of this material in the required "anti" configuration,[1] i.e., with all six nitrogen atoms of the three dmg^{2-} ligands coordinated to Co(III), was reported by Boston and Rose.[1a] These authors also reported the reaction of $K_3[Co(dmg)_3]$ with 2 equiv of the Lewis acid boron trifluoride to produce $[Co(dmg)_3(BF)_2]BF_4$, in which the tricyclic ligand cage is joined together at both ends by the formation of boron-oxygen bonds to form the *clathrochelate* shown below:

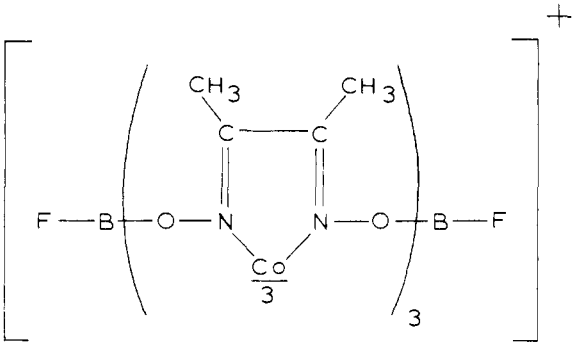

Of particular interest to this work was the fact that this low-spin, diamagnetic Co(III) complex could be readily reduced under mild conditions to the low-spin, paramagnetic Co(II)